Development of a High-Strength Zwitterionic Hydrogel to Combat Biofouling in Marine and Medical Applications

Joel MacArthur

A thesis

submitted in partial fulfillment of the

requirements for the degree of

Master of Science in Chemical Engineering

University of Washington

2019

Committee:

Shaoyi Jiang

Qiuming Yu

Program Authorized to Offer Degree:

Chemical Engineering

Abstract

Development of a High-Strength Zwitterionic Hydrogel to Combat Biofouling in Marine and Medical Applications

Joel MacArthur

Chair of the Supervisory Committee:
Professor Shaoyi Jiang
Department of Chemical Engineering

Biofouling is a phenomenon that targets nonnative objects in biological settings, which has detrimental economic effects on global industry, notably those operating in marine or medical environments. In our efforts to prevent biofouling in various applications, we have developed a biocompatible polymer that exhibits incredible hydrophilic and nonfouling properties in a range of host systems, while boasting impressive mechanical properties and bulk stability of the coating. In this study, the mechanical properties and antifouling performances of high-strength zwitterionic hydrogel sheets and microgel coatings were studied at length. Both materials showed substantially improved antifouling effects versus polydimethylsiloxane (PDMS) and glass control surfaces and still presented superhydrophilic surfaces after more than 2 months in aqueous environments. In addition, fouling that does occur on our surfaces can be easily removed if light cleaning is

performed at regular intervals. Consequently, these materials are viable options in many applications to negate the effects of biofouling.

TABLE OF CONTENTS

LIST OF FIGURES

Chapter 1. BACKGROUND

In the shipping industry, biofouling in the forms of biofilms and organisms such as barnacles leads to increases in the powering requirements for marine vessels from induced drag and increased displacements. Other unfavorable consequences from marine fouling are damage to marine structures, clogging of ship machinery and sea chests, and the transport of potentially invasive species [1]. In the medical field, biofouling in the forms of undesired blood clotting, biofilm formation, and protein adsorption can lead to failures of medical devices, increased costs, and additional surgical procedures [2]. Our research group is currently investigating the possibility of using zwitterionic double-network (ZDN) hydrogel sheets and microgel coatings to prevent fouling on marine and medical surfaces without reliance on toxic substances such as copper or biocides in marine applications, and without need for surface modification or application of antifouling coatings as is the case for most medical products [3]. In the medical field, surgical devices and implants are frequently developed from hydrophobic materials which have little defense against host attack of fouling organisms and therefore require further surface modification or functionalization prior to use. In contrast, our approach is to develop a multi-network hydrogel that has sufficient strength to be suitable for surgical applications while also exhibiting a hydrophilic barrier at the surface, conferring a stealth property to mitigate or stop host attack.

Marine fouling is typically described as a four-stage process. Within minutes of immersion in natural seawater, organic molecules such as proteins and polysaccharides bind to untreated surfaces through a combination of electrostatic and van der Waals interactions [4]. These molecules form a “conditioner film” which favors the adhesion of bacteria and single-celled algae starting around 24 hours. Within a week the third stage is initiated, and larger spores of microalgae populate the surface, forming a biofilm and offering functions such as nutrient transport and

protection from toxicants. In the final stage, larvae of marine macroorganisms adhere to the surface, only a couple weeks after the initial immersion of the surface. Fouling is split into two categories, hard fouling and soft fouling. Hard fouling consists of shelled organisms such as mollusks and barnacles, while soft fouling is comprised of biofilms formed on wetted surfaces by flora such as grasses and algae [4].

Biofouling in medical applications proceeds along a similar process in principle to that seen in the marine environment, but on a much smaller scale. When the host senses a change in physiological processes, it will activate defense processes that normally function to fend off the deleterious effects of bacteria, foreign bodies, and tissue injury [5]. Such a change could be driven by the addition of a surgical implant, the long-term intrusion of a catheter, or pairing a drug with a carrier matrix to which the host has already developed an adaptive immune response. In addition, if a medical device has insufficient strength to withstand the stresses inherent to normal use and fails, it may degrade and particles will separate from the implant, leading to foreign body response and fouling [5]. Even in a device with sufficient strength, biofouling can be initiated via foreign body response and can lead to the degradation or loss of function of the device. In cases where a host's immune response is inadequate to degrade these foreign objects via phagocytosis, the activation of exocytosis towards a surgical implant or device can lead to damage of healthy tissues and systems nearby [5]. Loss of device function and uncontrolled immune responses can lead to increased costs of services and can require additional surgeries in order to remove or replace implants. With each additional surgery, both the risk of infection and time of recovery increase substantially, placing greater impetus on researchers to develop materials that can function long-term within hosts without activation of immunological responses [6].

The goal of antifouling surfaces in the medical field is to prevent immunological response to the foreign object by making a surface that interacts minimally with the normal biological processes of the host. When it does interact, the material should have a molecular composition that can easily be processed by the body without inciting a larger inflammatory response [5]. In addition, whether the material is being used as a catheter tube, a pharmaceutical carrier, or a tissue engineering scaffold, it must be strong enough to handle the stresses characteristic to its primary function. The popular approach to accomplishing these objectives is to coat a hydrophobic device surface with a hydrophilic material without diminishing the mechanical properties of the bulk material [7]. The two methods commonly associated with this approach each have challenges. Using the "graft-to" method, it can be difficult to achieve sufficient surface packing densities or long-term stability of the surface coating, leading to surface fouling and failure; the "graft-from" method entails complicated reactions carried out in pristine environments, which is a significant obstacle when researchers desire to scale up the production of designed prototypes [8]. Some notable approaches to antifouling surfaces in recent history are poly-SB modified catheter tubing, diblock copolymers of PEG and cationic polycarbonate, and amphiphilic poly(2-methacryloyloxyethyl phosphorylcholine-co-3-methacryloyloxy-2-hydroxypropyl-4-oxybenzophenone (MPC)-*co*-MHPBP [9-11]. Our group is pursuing a different approach than the above by developing a homogeneous zwitterionic composite that in aqueous or blood environments establishes a strong hydrophilic barrier, obstructing fouling organisms from binding to the surface.

Zwitterionic polymers are polymers that have an equimolar number of anionic and cationic groups arranged evenly throughout their polymer chains [12]. Three of the distinguishing factors between different zwitterionic materials are 1) their choice of polymer backbone, 2) the ionic

groups included in their polymer structure, and 3) the distance separating positive and negative charges on each polymer chain [13]. One advantage of zwitterions is that they are biocompatible and hemocompatible, allowing them to blend in with their host environment and be degraded without a serious immune response when they fail [14]. In zwitterionic materials that can absorb water and present a hydrophilic layer at a protein-polymer interface, the water layer serves as both energetic and physical barrier and must be discharged from the surface before protein adhesion can occur [15]. In addition, steric resistance is provided from elasticity of the polymer surface, as proteins must compress polymer chains to approach before binding [16]. *Hydrogels* are polymeric materials that are hydrophilic and able to retain high percentages of water content at equilibrium. In our study, *microgels* are hydrogel sheets that have been structurally reduced by extruding them through mesh filters with micron-sized cross-sectional openings. *Double-network* (DN) hydrogels are a subset of hydrogels that are synthesized by soaking a completed hydrogel sheet (the first network) in another hydrogel's monomer solution (the second network). Once the first network has had sufficient time to absorb the second network solution, the composite material is polymerized resulting in a DN hydrogel sheet, a densely-packed matrix consisting of both the first and second network hydrogels. When both hydrogels in a double-network hydrogel are zwitterionic monomers, the product is called a zwitterionic double-network (ZDN) hydrogel. Double-network hydrogels have been shown by numerous studies to have much higher mechanical strengths than their respective first-network hydrogels, and by using zwitterionic monomers in balanced proportions, antifouling properties will also be observed [17]. One of the challenges to a successful nonfouling surface is that as soon as microorganisms have penetrated the hydrophilic layer and bound to the surface, the effectiveness of the water barrier can be greatly diminished and the performance of the entire area may begin to fail at an exponential rate [3]. Even aggregates of

dead bacteria or proteins at the surface layer act as an organic substrate for colonizing microorganisms to bind to and promote the fouling process. Thus, an antifouling surface must completely prevent the initial adhesion of the fouling proteins in its environment in order to experience long-term success. Alternatively, a material that greatly diminishes the binding interactions of fouling organisms permits the quick removal of fouling from any surface where even minimal shear forces are present. In this study, we present such a material with our design of a ZDN hydrogel sheet and corresponding microgel coating which both show exceptional results in antifouling applications. Comprehensive mechanical, fouling, and wettability studies confirm this material is strong and elastic, effective at maintaining a hydrophilic barrier to fouling organisms, and remarkably effective at shedding fouling organisms in the presence of low shear stresses. In addition, its ability to be applied either as a hydrogel sheet or microgel coating make it a prime choice for use in countless antifouling applications ranging from marine structures to medical tools and implants.

Chapter 2. EXPERIMENTAL MATERIALS AND METHODS

2.1 HYDROGEL SHEET PREPARATION

For the preparation of the hydrogels in this study, the following materials were obtained from Sigma-Aldrich: 2-Hydroxy-2-methylpropiophenone (1173) photo-initiator (CAS 7473985), [2-(Methacryloyloxy)ethyl]dimethyl-(3-sulfopropyl)ammonium hydroxide (SB) monomer (CAS 3637261), and N, N'-Methylenebis(acrylamide) (MBAA) crosslinker (CAS 110269). The hydrogels in this study were synthesized through a multi-stage free-radical polymerization. For the initial polymerization, first network poly{3-[3-(acrylamidopropyl)dimethylammonio]propionate} (pCB) hydrogel sheets were synthesized via photo polymerization using 1 M of CB, 4 mol% of

cross-linker MBAA, and 0.1 mol% of initiator 1173 in transparent glass sheet molds via 10 minutes of ultraviolet (UV) irradiation at a 312 nm wavelength and 90 watts of power. For all hydrogel syntheses, deionized (DI) water was used as the solvent. The mol% of initiator and crosslinker were calculated relative to the CB monomer weight, and to control the thickness of the first network, glass sheets were separated by a 1 mm polytetrafluoroethylene spacer. The monomer CB was synthesized in house through the reaction process outlined in an earlier publication from this research group [18].

To form the second network, the pCB hydrogel sheet was placed in the second network precursor solution containing 4 M of [2-(Methacryloyloxy)ethyl]dimethyl-(3-sulfopropyl)ammonium hydroxide (SB), 0.1 mol% of MBAA and 0.01 mol% of initiator 1173 for 24 hours. Once saturated with the precursor solution, the hydrogel was polymerized via 4 hours of UV irradiation at a 302 nm wavelength and 50 watts of power in a nitrogen-evacuated environment. Following the second polymerization, the pCB/pSB ZDN hydrogel sheets were transferred to aqueous solution for 24 hours to reach saturation in water. Mechanical strength studies were completed using numerous concentrations of the CB and SB monomers and MBAA crosslinker to determine the most marketable products from each of the possible first/second network combinations (pCB/pCB, pSB/pSB, pCB/pSB, pSB/pCB). Each hydrogel formulation was synthesized using the process outlined above with changes only to the monomers and their concentrations.

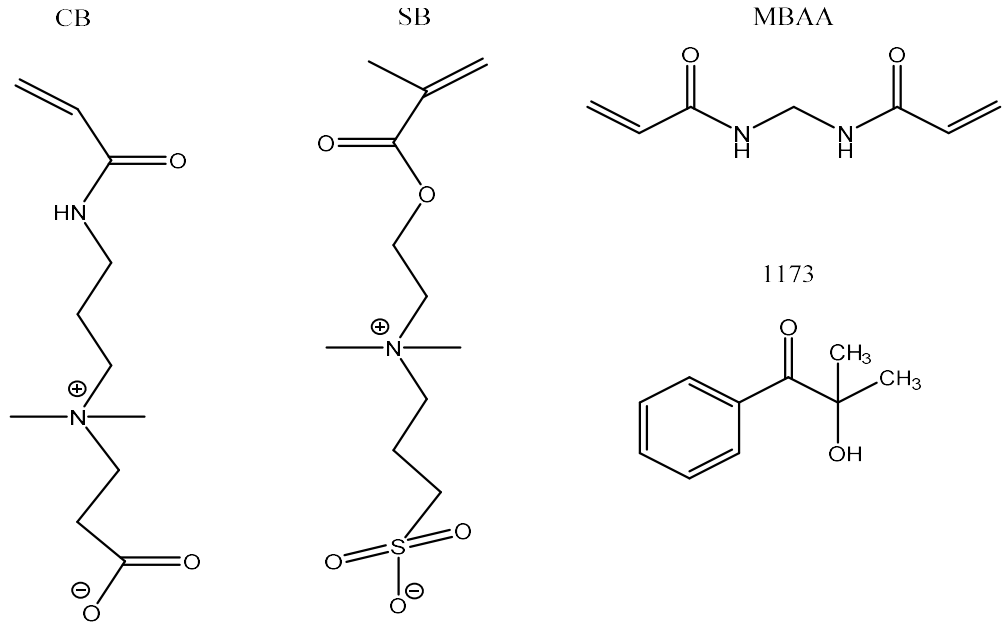

Figure 1. Reactants used in ZDN hydrogel synthesis

Microgels were created by extruding hydrogels through steel mesh (370 µm pores) using a stainless-steel piston and cylinder assembly. Hydrogel sheets were loaded into the press, strained through the filter 3 times to ensure uniformity of microgel size, and stored in airtight containers. The pCB/pSB material selected for microgel testing was chosen from the tested hydrogels because of its observed strength, elasticity, and hydrophilicity.

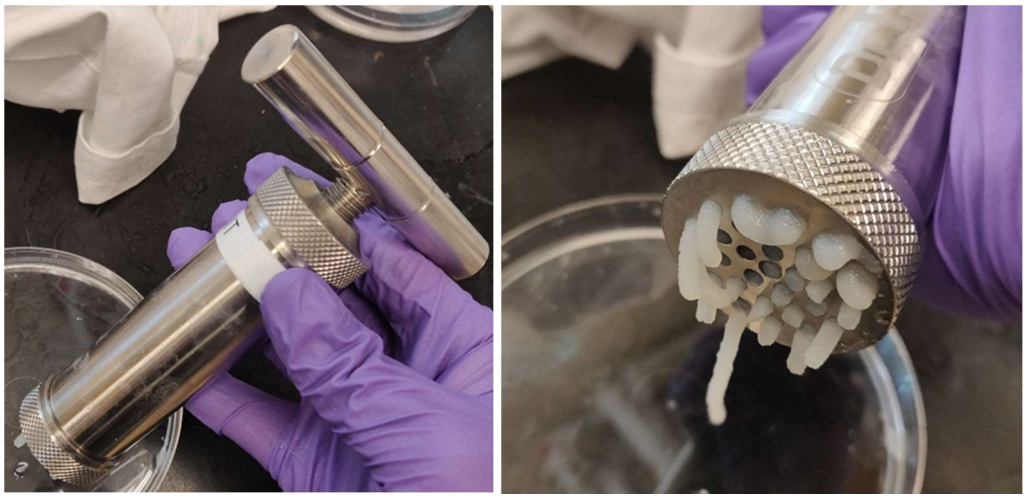

Figure 2. Microgel extrusion process. Hydrogel sheets were loaded into the press and forced through 370 µm pores using the piston and cylinder assembly

2.2 Hydrogel Sheet Characterization

Compressive tests were completed with a tensile-compressive mechanical tester (Instron 5543A, Instron Corp., Norwood, MA) with a 10 kN load cell to observe and annotate the mechanical properties of the ZDN hydrogel samples. For compressive tests, the crosshead speed was preset at 1 mm min^{-1}. The cylindrical hydrogel samples were cut with diameters of 5 mm and heights ranged from 1-2 mm. Average data was calculated by testing at least five hydrogel discs for each hydrogel material. A group of 8 materials of varying monomer and crosslinker concentrations was tested from each $1^{st}/2^{nd}$ hydrogel network combination (pCB/pCB, pSB/pSB, pCB/pSB, pSB/pCB), and the strongest material from each category was kept for comparison.

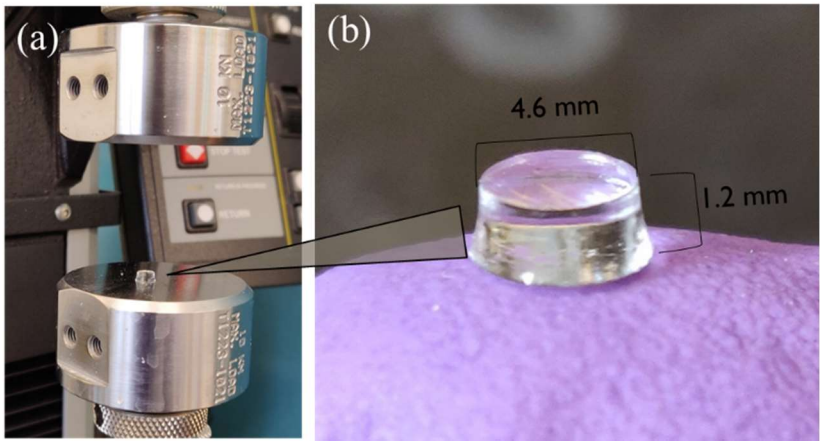

Figure 3. (a) Instron 5543A tensile-compressive mechanical tester loaded with pCB/pSB hydrogel disc and (b) Average pCB/pSB hydrogel disc dimensions used for mechanical testing. Disc heights varied between hydrogels due to swelling behavior differences between materials

After the 5mm diameter ZDN hydrogel cylinders were photo-polymerized, their as-prepared volumes (V_p) were calculated, and the samples were then soaked in deionized water for 48 h to reach saturation. After removing the discs and blowing off all residual surface water with nitrogen gas, the volumes and masses of the saturated hydrogel cylinders (V_s, M_s) were then measured. The cylinders were placed in an oven at 120°C for 24 h to remove all water content,

and the masses of the dried cylinders (M_d) were recorded. Equilibrium water content (EWC) for each material was calculated through gravimetric comparison of the water-saturated (M_s) and dry polymer states (M_d) using the equation EWC = 100% x (M_s – M_d)/M_s. The equilibrium swelling ratios (ESR) were calculated through the volumetric comparison of each hydrogel sample at the polymerized (V_p) and water-saturated states (V_s) using the equation ESR = 100% x (V_s/V_p).

Contact angles of water on the pCB/pSB hydrogel in a standard atmosphere were observed using pCB/pSB hydrogel sheets mounted on fiberglass substrates. First, pCB/pSB hydrogel sheets were soaked in DI water for 48 h to reach saturation. The hydrogel sheets were removed from the DI water, and the water lying on the hydrogel surface was dispersed via compressed air. Finally, a 5 µL drop of DI water was set on the surface. For contact angles of air bubbles on pCB/pSB hydrogel sheets submerged in deionized water, a DI water-saturated pCB/pSB sheet was submerged in DI water and a 15 uL bubble of atmospheric air was placed under the sheet. Hydrophilicity of pCB/pSB microgel coatings was determined by the visual assessment of whether water was held on or repelled from the coating surface when removed from an aqueous environment. Gravitational force was introduced to the surface water by lifting the sample at an inclined angle.

2.3 Fouling Tests

Biofouling tests were carried out in collaboration with Newcastle University in the UK. Once prepared, hydrogel sheets and microgel coatings were attached to fiberglass substrates with cyanoacrylic adhesive and stored in artificial saltwater (ASW) for shipment. Photos are provided in Appendix A of the hydrogel sheets and Appendix B of the microgel coatings prior to the fouling tests. For the hydrogel testing, personnel at Newcastle University cultured cells of *N. incerta* in F/2 medium supplied in 250 mL conical flasks. After 3 days, the cells reached log phase growth.

Cells were then rinsed 3 times in fresh F/2 medium before harvesting, and were diluted to give a suspension with a chlorophyll content of ~0.2 μg mL^{-1}. Cells were settled on three replicate-coated slides of each sample, in individual quadriPERM® dishes containing 15 mL of suspension, at roughly 20°C. After 2 hours of exposure, the slides were subject to 5 minutes of agitation on an orbital shaker (60 rpm) and rinsed with seawater to remove any cells that had not attached. While the samples were still wet, images were taken of three slides of each type with an analysis system included with a fluorescence microscope. Cells were identified through the auto-fluorescence of chlorophyll. Counts were completed for 30 fields of view of 0.56 mm^2 slices for each sample. Following the initial counts, the slides were placed in a water channel for 5 minutes, undergoing 26 Pa of shear stress. After this cleaning, the samples were counted again using the same process described above.

For the microgel biofouling tests, zoospores were harvested from mature plants of *U. linza*, and a suspension of zoospores (15 mL; $7.5x10^5$ spores mL^{-1}) was distributed to individual compartments of quadriPERM dishes that held the sample slides. After 45 minutes stored in darkness at 20ºC, the slides were viewed under the microscope to establish how much settlement had taken place. The samples were gently rinsed under seawater to remove unsettled spores following the method discussed for hydrogel testing above. After the washing process, the samples were again observed through the microscope to conduct spore counts on the samples. The hardware and parameters used for these counts were the same as for the hydrogel testing outlined above. Lastly, the slides were exposed to a shear stress of 52 Pa in the turbulent flow water channel and recounted as described above.

Chapter 3. RESULTS AND DATA

3.1 Mechanical and Swelling Data of Hydrogels

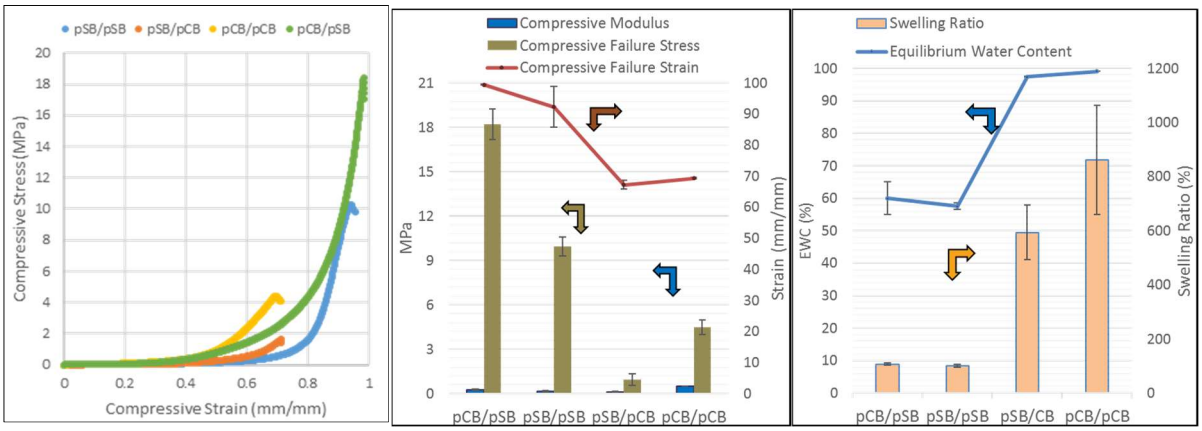

Figure 4. (a) Compressive load curves, (b) Compressive modulus, fracture stress and fracture strain, and (c) Equilibrium swelling ratios and equilibrium water contents of pCB/pSB, pSB/pSB, pSB/pCB, and pCB/pCB ZDN hydrogels. 1st/2nd network compositions were 1-4-0.1/4-0.1-0.01 for pCB/pSB and pSB/pSB, and 1-4-0.1/4-0.2-0.01 for pSB/pCB and pCB/pCB.

The pCB/pSB ZDN hydrogel sheets saturated in DI water were by far the strongest material with an average compressive fracture stress more than 18 MPa and were unbroken while exhibiting up to 99% compressive strain. The load drop shown for the pCB/pSB ZDN hydrogels in Figure 4(a) is not due to compressive failure; instead, the hydrogels became mobile and slipped out of the compressive testing apparatus before failure was reached. In fact, no pCB/pSB samples showed signs of compressive failure at loads around 18 MPa. At equilibrium in DI water, the pCB/pSB ZDN hydrogel had low swelling with a 7% volume increase compared to that of the pCB/pSB ZDN hydrogel immediately after polymerization, and it had an EWC just over 60%. The pCB/pCB ZDN hydrogel had the highest swelling ratio at over a 725% volume increase compared to its post-polymerization volume and had an equilibrium water content over 99%, but its compressive failure stress and strain only averaged 4.5 MPa and 69% respectively. The remaining strength and swelling observations for the most durable hydrogels from each first/second hydrogel network

combination are shown in Figure 4 above. Because these ZDN hydrogels draw their strength and elasticity from the ability of the second-network material to distribute local stresses throughout the first-network backbone, the monomers should be arranged in such a way that there is maximum absorption of the second network precursor by the polymerized first network. This can be quantified through the volumetric change of the first network when immersed in the second network precursor solution. In addition, although the penetration of water is helpful in maintaining the hydrophilic boundary layer at the hydrogel surface, it is detrimental to the mechanical strength of the bulk hydrogel because it interrupts the second network that has penetrated throughout the first network matrix and reduces its ability to redirect local stresses. In this study, the arrangement of monomers that best achieved this balance was CB as the first-network and SB as the second-network hydrogel.

3.2 pCB/pSB Microgel Coatings

Our pCB/pSB microgels exhibited super-hydrophilicity in DI water. Photos of the microgel coating samples are provided in Appendix B. Adhesive layers of cyanoacrylic glue were introduced on the fiberglass substrate to improve the adhesion of the microgel to the surface, resulting in a thin microgel coating relative to the thickness of the pCB/pSB hydrogel sheets. The high water retention that is innate to its parent hydrogel can be perceived visually in the microgel as it is removed from immersion in DI or artificial saltwater. Also, over periods of several months stored in artificial saltwater, the microgel coating has shown the ability to remain intact and stable on the substrate surface. Because of the material's long-term stability and hydrophilic behavior, we also sent ZDN pCB/pSB microgels to undergo fouling tests.

3.3 FOULING DATA

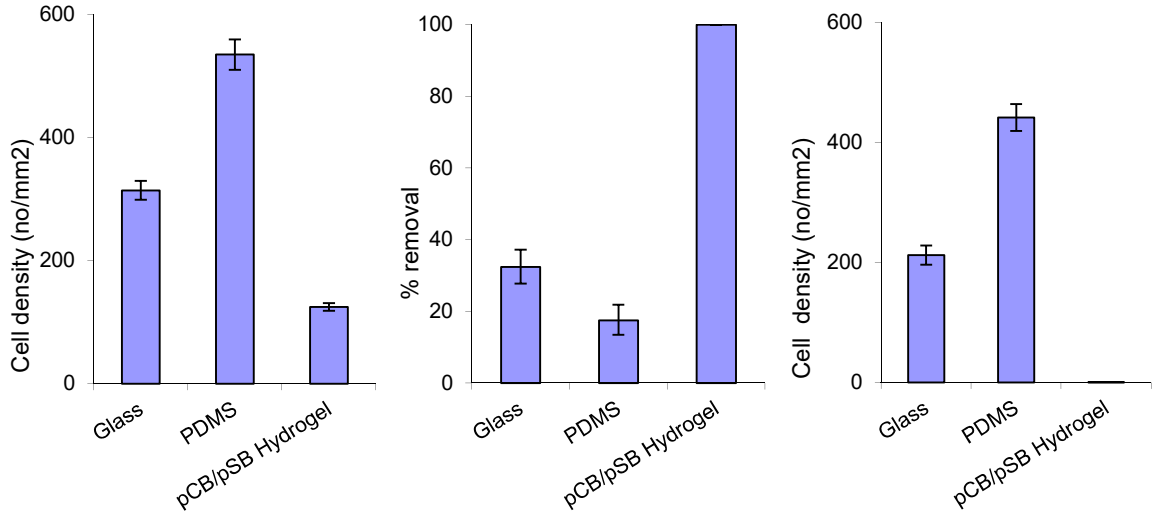

Figure 5. (a) The density of attached diatoms on zwitterionic hydrogels after 2 hours followed by washing. Each point is the mean from 90 counts from 3 replicate slides. Bars show 95% confidence limits (b) Percent removal of diatoms from zwitterionic hydrogels due to a shear stress of 26Pa. Each point is the mean from 90 counts from 3 replicate slides. Bars show 95% confidence limits derived from arc-sine transformed data (c) The density of diatoms remaining on zwitterionic hydrogels after exposure to a shear stress of 26Pa. Each point is the mean from 90 counts on 3 replicate slides. Bars show 95% confidence limits.

The fouling results for the 1-4-0.1/4-0.1-0.01 pCB/pSB hydrogel are shown in Figure 5. After 2 hours of exposure to *N. incerta* populations, our hydrogel surface showed substantially lower fouling density than those observed on the glass and PDMS surfaces. In addition, the minor fouling that did occur on the hydrogels was much weaker than that on the glass and PDMS reference surfaces, and all of it was removed by the 26 Pa stress in the water channel. Even prior to this washing process, cells that were very weakly attached to the surface were inadvertently removed by the gentle washing stage via the orbital shaker. Only one measurable shear stress was used to remove the attached diatoms in this procedure (26 Pa), and it is very possible that the cells would have still detached from using substantially lower hydrodynamic forces.

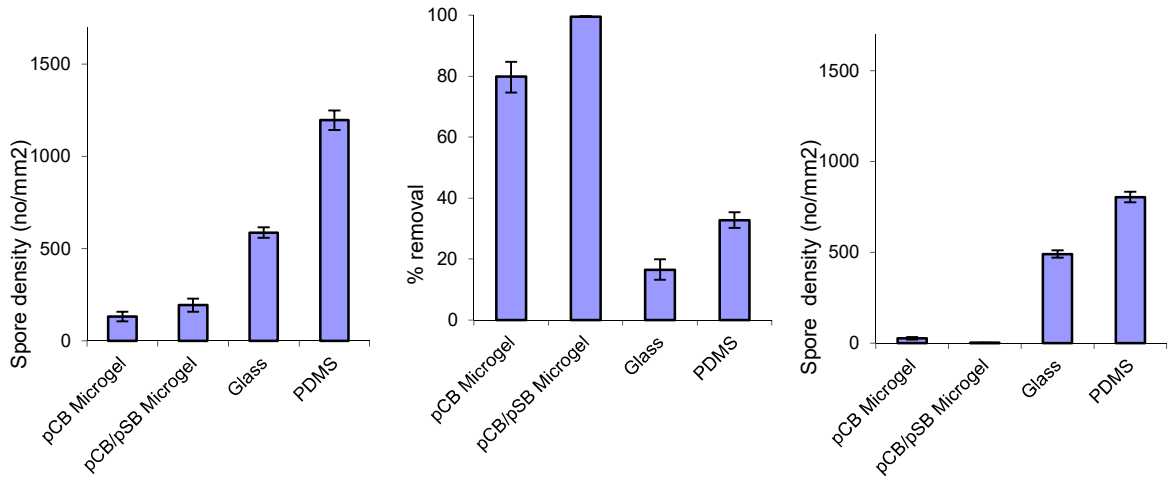

Figure 6. (a) The density of attached spores on the zwitterionic hydrogel coatings after 3 hours' settlement. Each point is the mean from 90 counts on 3 replicate slides. Bars show 95% confidence limits. (b) The removal of spores from zwitterionic hydrogel coatings due to exposure to a shear stress of 52Pa. Each point is the mean from 90 counts on 3 replicate slides. Bars show 95% confidence limits derived from arc-sine transformed data. (c) Final density of attached spores on zwitterionic hydrogel coatings after washing and exposure to a shear stress of 52Pa. Each point is the mean of 90 counts on 3 replicate slides. Bars show 95% confidence limits.

The fouling results for the microgel samples are shown above in Figure 6. Spore counts taken prior to washing showed that there was spore attachment on each of the tested surfaces, seen in Figure 6(a). The pCB/pSB microgel coating is shown as the second column from the left on each of the graphs above, and a single-network 1-4-0.1 pCB microgel coating is shown by the leftmost column. All of the spore settlement that was observed on the ZDN microgel surface was removed by the washing process, an identical result to the data observed for its hydrogel counterpart in Figure 5. It is apparent that the pCB/pSB microgel coatings outperformed the glass and PDMS surfaces in initial fouling density, and were the best performers in spore density after the washing of all the tested samples.

CHAPTER 4. DISCUSSION OF RESULTS

4.1 Strength Improvements of pCB/pSB from pCB/pCB and pSB/pSB

The mechanical strength advantage of the pCB/pSB hydrogels in this study is readily apparent from the graphs given in Figure 4. The only tested material comparable to its 18 MPa failure stress and 99% failure strain was the pSB/pSB hydrogel with around 10 MPa failure stress and 92% failure strain. Both of these are also dramatically improved from their respective single-network hydrogels, a behavior that is mostly due to the fluidity of ductile second-networks distributing localized stresses through the more crosslinked and brittle first network structure [17]. This behavior contrasts with the common understanding that strength improvements would strictly be a result of molecular interactions between the two networks or rigidity from increased crosslinking. These data and fundamental understandings of the ZDN hydrogel behavior affirm that our material is both elastic and highly durable, which will make it suitable for many different applications that require it to be molded, cut, or adhered to a surface. Due to its impressive mechanical strength and hydrophilic behavior in aqueous environments, we focused on this material through the remainder of the study for antifouling and microgel surface coating tests.

4.2 Equilibrium Water Content and Surface Wettability

The pSB/pCB and pCB/pCB hydrogels had substantial water absorption before reaching equilibrium in DI water, but their low failure stresses and strains made them irrelevant to the applications we were focusing on. Despite the relatively low absorption of water by volume into the pCB/pSB hydrogels, their robust hydrophilicity in aqueous environments is evident from their contact angles with air and water shown Figure 7. Although these contact angle assessments are not exact, the hydrophilicity of the pCB/pSB surface can easily be distinguished visually by the

very low water contact angle in Figure 7(a) and the high air contact angle in Figure 7(b). In both scenarios, the pCB/pSB hydrogel was saturated in DI water prior to the test, which is the same condition it will be prepared in prior to most of its intended applications. The high water retention and hydrophilic behavior that was innate to the pCB/pSB hydrogel can be also be perceived in the pCB/pSB microgel. When a material coated with the microgel is removed from an aqueous environment, a water film is preserved on the microgel surface and can be perceived visually. Due to the surface roughness of these coatings, the water and air contact angle could not be depicted visually as was done for the hydrogel.

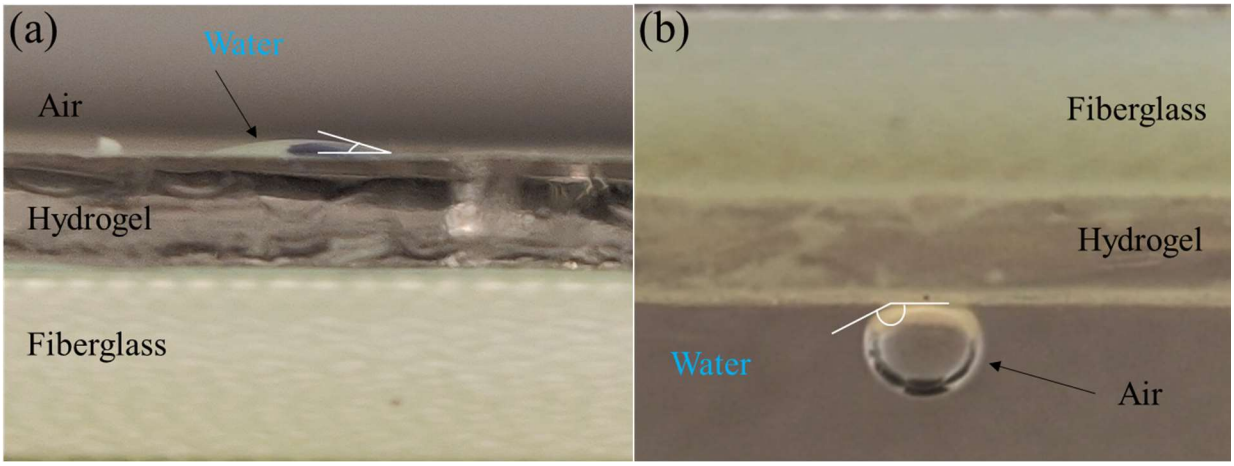

Figure 7. (a) 5 µL drop of deionized water placed on pCB/pSB hydrogel mounted on fiberglass surface. Prior to testing, surface water was removed with pressurized air. (b) 15 µL bubble of atmospheric air held underneath pCB/pSB hydrogel mounted on green fiberglass surface. Sample was submerged in deionized water. Contact angle estimations are shown in white on both images.

Because zwitterionic materials draw their antifouling performance from the hydrophilic barrier formed at their surface, the hydrophilicity of pCB/pSB can also in part be inferred from its fouling performance discussed below. And finally, a reasonable affinity towards water could be predicted from the molecular structures of the zwitterionic monomer units CB and SB shown in Figure 1. Both molecules present polar ester groups as well as separation of opposite charges

in their geometries, supporting the assumption that their composite would show at least a modicum of hydrophilic behavior.

4.3 Microgel Stability and Hydrophilicity

As discussed earlier, the strength of pCB/pSB hydrogel sheets is due to the ability of the pSB second-network to evenly distribute localized stresses throughout the stiff pCB first-network matrix. When the ZDN hydrogel was extruded through the micron-sized filter, the resultant structure is composed of pCB and pSB chains that remain tangled and crosslinked but are no longer capable of the long-range interactions that were made possible by the tightly packed matrix of the ZDN hydrogel. The reduced structure allows the microgel to form a thinner coating than the hydrogel, and the fouling tests showed no observable effects on the fouling performance as a result of the structural change. This modified format of the pCB/pSB material also makes it behave similarly to a liquid, making it feasible for the coating to be applied via spraying, brushing, or in the case of internal surfaces such as medical tubing, application by flowing.

4.4 Fouling Performance

The antifouling performance of the pCB/pSB hydrogel sheets in this study was conclusively better than that of PDMS from the data given in Figure 5. The data shows that fouling did take place, but it was extremely weak and was easily removed from the surface by the gentle washing process that was used. These results in conjunction with the contact angle observations made above suggest that the pCB/pSB hydrogels we synthesized successfully promote a water barrier when in aqueous environments, allowing them to repel fouling species and radically weaken the surface interactions of proteins that can attach to the surface. The pCB/pSB microgel was also subjected to the fouling tests and performed exceptionally well. Spore settlement densities

on the pCB/pSB microgel coatings were also much lower than those on the glass and PDMS surfaces, shown by the data in Figure 6. In addition, the adhesion of spores to the surfaces was weak and they were easily removed by the 52 Pa shear stress from the flow channel. Future testing could compare the performance of our material to other antifouling surfaces and at longer exposure times, but as it stands, our material is thoroughly effective as an antifouling material. Combined with its strength, this makes it suitable for many applications in the medical field. Our hydrogel can be molded, cut, or adhered to a surface, and the microgel can be sprayed, brushed, or flowed onto internal surfaces, making this material in its two forms highly marketable as an acceptable material that can be used in countless antifouling applications.

CHAPTER 5. CONCLUSIONS

5.1 PRACTICAL APPLICATIONS

There are a wide range of practical applications that we believe are possible with the ZDN hydrogel and microgels that we have developed. In the medical field, the hydrogels could be molded to function as catheters or other medical tubing, they could be used as tissue scaffolds to assist native tissue regrowth, or even used as an alternative to the current composition of contact lenses. If modified to facilitate controlled release of a payload, these hydrogels could also be used either in the pharmaceutical or implant fields to arrange controlled delivery of nanoparticles, biomolecules, or cells inside patients. Alternatively, in applications to combat marine biofouling, we believe that the hydrogels or microgels can function as antifouling coating surfaces on manmade objects in the marine environment ranging from oceangoing vessels to stationary structures like piers or buoys. Some more possibilities we could explore are applying them as

internal coatings of piping within ship systems such as raw water heat exchangers or reverse osmosis units, or on external ship sensors like fathometers or sonar transmitters.

5.2 Future Direction

In applications as a surface coating, we are investigating different methods to accomplish strong adhesion to hydrophobic surfaces such as PDMS, fiberglass, and steel in order to impart these substrates with the antifouling properties of these durable ZDN hydrogels and microgels. So far, strong adhesion to substrates has been accomplished primarily via cyanoacrylic adhesives but they have relatively fast cure times, sometimes making it difficult to effectively mate samples to their substrates. Investigating new concentrations of our ZDN hydrogels and how they interact with a variety of adhesives can make this product more practical and therefore marketable to everyday users. In addition, we believe improvements to our synthesis procedures can be made to further increase the mechanical strengths of our ZDN hydrogels. Adjustments to the reactants and conditions of the polymerization processes will increase the failure strength and elasticity of our product, making it stand out even more as a long-term solution to biofouling scenarios. For future fouling tests, a longer timescale than 3 hours would show whether the fouling-release properties of the pCB/pSB hydrogel and microgel are still possible when fouling organisms have had a longer time to populate and adhere to the coating surface. In addition, once a practical method has been derived to scale-up production of the hydrogel sheets, it would be instructive to test these materials alongside the pCB/pSB microgel as antifouling coatings in marine environment field tests.

BIBLIOGRAPHY

[1] NAVSEA US Naval Sea Systems Command. Environmental assessment of fleetwide use of organotin antifouling paint. NAVSEA. Washington, DC, 1984:128.

[2] Nair, and Laurencin. "Biodegradable Polymers as Biomaterials." *Progress in Polymer Science*, vol. 32, no. 8, 2007, pp. 762–798.

[3] Banerjee, Indrani, et al. "Antifouling Coatings: Recent Developments in the Design of Surfaces That Prevent Fouling by Proteins, Bacteria, and Marine Organisms." *Advanced Materials*, vol. 23, no. 6, 2011, pp. 690–718.

[4] Almeida, et al. "Marine Paints: The Particular Case of Antifouling Paints." *Progress in Organic Coatings*, vol. 59, no. 1, 2007, pp. 2–20.

[5] Ratner, B. D., et al. *Biomaterials Science : an Introduction to Materials in Medicine*. 3rd ed., Academic Press, 2013.

[6] Campoccia, D., Montanaro, L., & Arciola, C. R. (2006). *The significance of infection related to orthopedic devices and issues of antibiotic resistance.* Biomaterials , 27 (11), 2331– 2339.

[7] Hung, Hsiang-Chieh, et al. "A Coating-Free Nonfouling Polymeric Elastomer." *Advanced Materials*, vol. 29, no. 31, 2017, p. n/a.

[8] Wong, Ieong, and Chih-Ming Ho. "Surface Molecular Property Modifications for Poly(Dimethylsiloxane) (PDMS) Based Microfluidic Devices." *Microfluidics and Nanofluidics*, vol. 7, no. 3, 2009, pp. 291–306.

[9] R. S. Smith, Z. Zhang, M. Bouchard, J. Li, H. S. Lapp, G. R. Brotske, D. L. Lucchino, D. Weaver, L. A. Roth, A. Coury, J. Biggerstaff, S. Sukavaneshvar, R. Langer, C. Loose, *Sci. Transl. Med.* **2012**, *4*, 153ra132.

[10] Ding, X, et al. "Antibacterial and Antifouling Catheter Coatings Using Surface Grafted PEG-b-Cationic Polycarbonate Diblock Copolymers." *Biomaterials*, vol. 33, no. 28, 2012, pp. 6593–6603.

[11] X. Lin, K. Fukazawa, K. Ishihara, *ACS Appl. Mater. Interfaces* **2015**, *7*, 17489.

[12] Dobrynin, Andrey V., et al. "Polyampholytes." *Journal of Polymer Science Part B: Polymer Physics*, vol. 42, no. 19, 2004, pp. 3513–3538.

[13] Mi, Luo, and Shaoyi Jiang. "Integrated Antimicrobial and Nonfouling Zwitterionic Polymers." *Angewandte Chemie International Edition*, vol. 53, no. 7, 2014, pp. 1746–1754.

[14] Chen, et al. "Surface Hydration: Principles and Applications toward Low-Fouling/Nonfouling Biomaterials." *Polymer*, vol. 51, no. 23, 2010, pp. 5283–5293.

[15] Chen, Shengfu, et al. "Strong Resistance of a Thin Crystalline Layer of Balanced Charged Groups to Protein Adsorption." *Langmuir : the ACS Journal of Surfaces and Colloids*, vol. 22, no. 19, 2006, pp. 8186–91.

[16] Jeon, et al. "Protein—Surface Interactions in the Presence of Polyethylene Oxide: I. Simplified Theory." *Journal of Colloid And Interface Science*, vol. 142, no. 1, 1991, pp. 149–158.

[17] Gong, et al. "Double-Network Hydrogels with Extremely High Mechanical Strength." *Advanced Materials*, vol. 15, no. 14, 2003, pp. 1155–1158.

[18] Sijun, Liu, and Jiang Shaoyi. "Chemical Conjugation of Zwitterionic Polymer Protects Immunogenic Enzyme and Preserves Activity with No Detectable Polymer-Specific Antibody Response." *Frontiers in Bioengineering and Biotechnology*, vol. 4, 2016, pp. Frontiers in Bioengineering and Biotechnology, 2016, Vol.4.

APPENDIX A

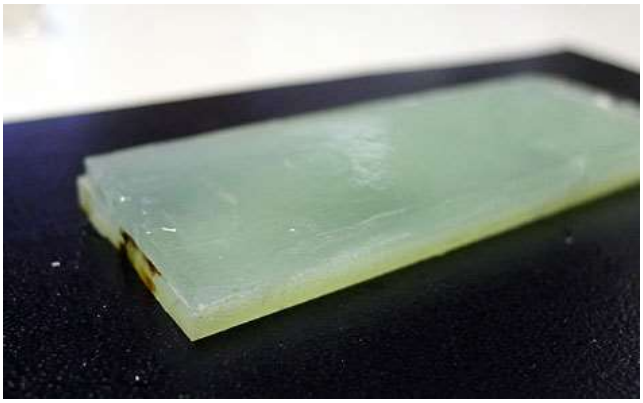

Figures A1 and A2. Hydrogel coating mounted on fiberglass slide.

APPENDIX B

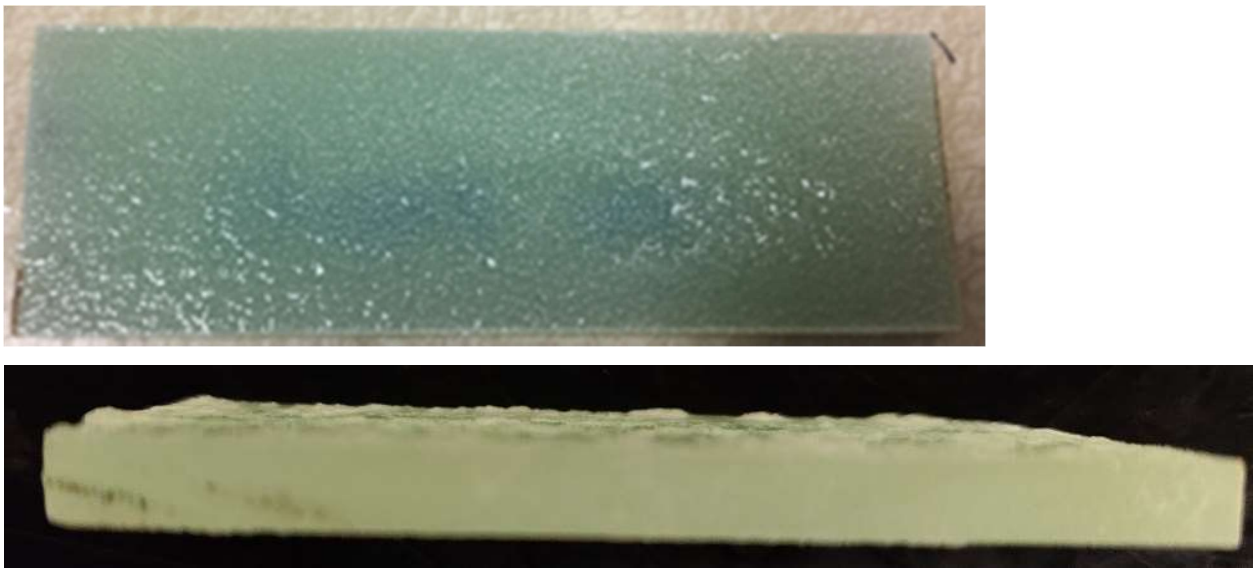

Figures B1 and B2. Microgel coating mounted on fiberglass slide.